

Electrochemical Synthesis and Characterization of a Series of Fluoro-Substituted Phenylene-2-thienyl Polymers

J. G. Killian, Y. Gofer, H. Sarker, T. O. Poehler, and P. C. Searson*

Department of Materials Science and Engineering, The Johns Hopkins University,
Baltimore, Maryland 21218

Received November 5, 1998. Revised Manuscript Received January 14, 1999

A series of electronically conducting polymers based on fluorine-substituted phenylene thienyl have been synthesized. The series includes poly-1,4-bis(2-thienyl)benzene (pTHB), poly-1,4-bis(2-thienyl)-2-fluorobenzene (pTFP), poly-1,4-bis(2-thienyl)-2,5-difluorobenzene (pTF2P), and poly-1,4-bis(2-thienyl)-2,3,5,6-tetrafluorobenzene (pTF4P). Thin films of the polymers were deposited by electropolymerization from solutions of the monomer and the doping properties characterized using electrochemical techniques. The polymers pTHB, pTFP, and pTF2P, exhibited reversible p-doping and n-doping with doping densities in the range of 0.15–0.45 electrons per monomer unit for p-doping and 0.12–0.18 electrons per monomer unit for n-doping. Secondary batteries were fabricated using these π -conjugated polymers as cathode and poly-3-(3,4,5-trifluorophenyl)thiophene (pTFPT) as the anode. On discharge, the cells exhibited an average potential of 2.75 V and charge capacities of 15–20 mA h g⁻¹, based on the polymer mass and a 100% depth of discharge.

Introduction

Electronically conducting polymers are a novel class of materials that exhibit many unique chemical, electrical, and optical properties. The conductivity of these materials can be controlled by partial oxidation (p-doping) or partial reduction (n-doping) of the neutral (semiconducting) polymer. The oxidation or reduction of the polymer is coupled with the transport of charge compensating ions into or out of the film, giving rise to the term doping. The change in the electronic structure associated with the doping process usually results in changes in the optical properties of the polymer. The band gap associated with the neutral state is typically in the range of 2–3 eV, so the potential difference between the conducting oxidized and reduced states is expected to be of similar magnitude.^{1,2} Repeated cycling between neutral and conducting states can be used for charge storage and optical switching. Other applications for these materials include integrated optoelectronic devices,^{3,4} luminescent devices,^{5,6} sensors,^{7,8} and charge

storage devices such as supercapacitors⁹ and rechargeable batteries.¹⁰

Polythiophene and polyparaphenylene are of particular interest since they are among the few electronically conducting polymers that exhibit reversible p-doping and n-doping. Modification of the monomer repeat unit or substitution of functional groups onto the polymer backbone can be used to achieve molecular level control of the structure and properties of the polymer. Substitution of thiophenes with a phenyl group^{11,12} or fluoro-phenyl group^{13–15} has been shown to yield improved n-doping performance. In previous work^{16,17} we have reported a doping density of 0.26 electrons per monomer unit and a cycle-to-cycle stability of 53.4% (charge retained over 100 cycles) for n-doping of poly-3-(3,4,5-trifluorophenyl)thiophene. Polyparaphenylene exhibits relatively high doping density and high stability; doping densities of 0.4 electrons per monomer unit have been reported in the literature.^{18,19}

Increasingly, attention has focused on the synthesis of multiple ring monomers.^{20,21} In this work we report

(1) Evans, G. P. In *Advances in Electrochemical Science and Engineering*; Gerischer, H., Tobias, C. W., Eds.; VCH Publishers: Amsterdam, 1990; Vol. 1.

(2) Shacklette, L. W.; Baughman, R. H.; Murthy, N. S. *Bull. Am. Phys. Soc.* **1983**, *28*, 320.

(3) Sirringhaus, H.; Tessler, N.; Friend, R. H. *Science* **1998**, *280*, 1741.

(4) Drury, C. J.; Mutsaers, C. M. J.; Hart, C. M.; Matters, M.; de Leeuw, D. M. *Appl. Phys. Lett.* **1998**, *73*, 108.

(5) Yang, Y.; Heeger, A. J. *Appl. Phys. Lett.* **1994**, *64*, 1245.

(6) Carter, J. C.; Gizzi, I.; Heeks, S. K.; Lacey, D. J.; Latham, S. G.; May, P. G.; Ruiz de los Paños, O.; Pichler, K.; Towns, C. R.; Wittmann, H. F. *Appl. Phys. Lett.* **1997**, *71*, 34.

(7) Fortier, G.; Brassard, E.; Belanger, D. *Biosensors Bioelectronics* **1990**, *5*, 473.

(8) Bartlett, P. N.; Whitaker, R. G. *J. Electroanal. Chem.* **1987**, *224*, 27.

(9) Carlberg, J. C.; Inganäs, O. *J. Electrochem. Soc.* **1997**, *144*, L61.

(10) Novák, P.; Müller, K.; Santhanam, K. S. V.; Haas, O. *Chem. Rev.* **1997**, *97*, 207.

(11) Roncali, J. *Chem. Rev.* **1997**, *97*, 173.

(12) Roncali, J. *Chem. Rev.* **1992**, *92*, 711.

(13) Roncali, J.; Youssouffi, H. F.; Garreau, R.; Garnier, F.; Lemaire, M. *J. Chem. Soc., Chem. Commun.* **1990**, 414.

(14) Rudge, A.; Raistrick, I.; Gottesfeld, S.; Ferraris, J. P. *Electrochim. Acta* **1994**, *39*, 273.

(15) Rudge, A.; Raistrick, I.; Gottesfeld, S.; Ferraris, J. P. *J. Power Sources* **1994**, *47*, 89.

(16) Sarker, H.; Gofer, Y.; Killian, J. G.; Poehler, T. O.; Searson, P. C. *Synth. Met.* **1997**, *88*, 176.

(17) Gofer, Y.; Killian, J. G.; Sarker, H.; Poehler, T. O.; Searson, P. C. *J. Electroanal. Chem.* **1998**, *443*, 103.

(18) Shacklette, L. W.; Toth, J. E.; Murthy, N. S.; Baughman, R. H. *J. Electrochem. Soc.* **1985**, *132*, 1529.

(19) Satoh, M.; Tabata, M.; Kaneto, K.; Yoshino, K. *Jpn. J. Appl. Phys.* **1986**, *25*, L73.

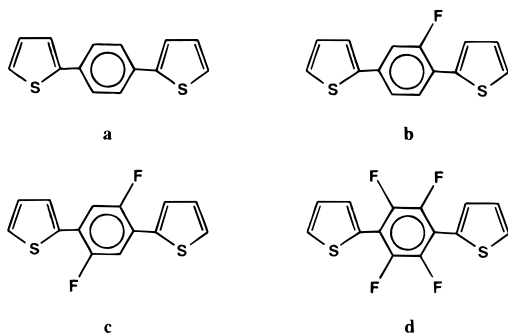


Figure 1. Molecular structure of the four monomers: (a) 1,4-bis(2-thienyl)benzene (THB), (b) 1,4-bis(2-thienyl)-2-fluorophenylene (TFP), (c) 1,4-bis(2-thienyl)-2,5-difluorophenylene (TF2P), and (d) 1,4-bis(2-thienyl)-2,3,5,6-tetrafluorophenylene (TF4P).

on the doping properties of a series of fluorine-substituted phenylene thienyl polymers including poly-1,4-bis(2-thienyl)benzene (pTHB), poly-1,4-bis(2-thienyl)-2-fluorobenzene (pTFP), poly-1,4-bis(2-thienyl)-2,5-difluorobenzene (pTF2P), and poly-1,4-bis(2-thienyl)-2,3,5,6-tetrafluorobenzene (pTF4P).

Experimental Section

General. All experiments were conducted in a glovebox maintained with an argon (Welders Specialty Gases and Cryogenics, 99.998% pure) atmosphere at room temperature. Benzonitrile (Aldrich, HPLC), distilled over CaH_2 under reduced pressure, was stored over activated molecular sieves. Propylene carbonate (PC, Burdick and Jackson, chromatography grade), methylene chloride (Aldrich, chromatography grade), and tetrahydrofuran (THF, Burdick and Jackson, chromatography grade) were stored over molecular sieves. AgClO_4 (ACS) was dehydrated for 48 h under dynamic vacuum at 100 °C. Ferrocene (Aesar, recrystallized) was used as received. Tetrabutylammonium tetrafluoroborate (TBABF_4 , Sachem, electrometric grade) was dehydrated for 48 h under dynamic vacuum at 125 °C. Residual water in the solutions was monitored periodically using a Metrohm Karl Fischer 684 KF Coulometer and was routinely lower than 20 ppm.

Potentials were measured versus a Ag^+/Ag reference electrode fabricated by inserting a silver wire into a tube with a Vycor tip containing a solution of 0.1 M AgClO_4 + 0.25 M TBABF_4 in PC. The reference electrode was calibrated with respect to the ferrocene/ferrocene (Fc^+/Fc) redox couple prior to each experiment.²² All potentials reported here are with respect to the Fc^+/Fc redox couple. The potential of the Ag^+/Ag reference electrode was about 0.4 V with respect to the Fc^+/Fc couple and about 3.65 V versus the Li^+/Li reference.

Monomers. The synthesis of the four monomers has been reported elsewhere.²³ The molecular structures of the monomers are shown in Figure 1. Prior to use, further dehydration of the monomers was carried out under dynamic vacuum at 40–100 °C.

Polymerization Potential. All electrochemical measurements were performed in a three-compartment glass cell with a Luggin capillary in which the working electrode compartment was isolated from the two counter electrode compartments by fine glass frits.¹⁷ A platinum disk (Aesar, 99.99%), 1.3 cm in diameter, served as the working electrode and two Pt meshes, each 2 cm^2 , served as the counter electrodes. This

design ensured the deposition of uniform polymer films and highly reproducible results.¹⁷

For the determination of the electropolymerization potential, the working electrode compartment was filled with a solution of 0.1 M monomer + 0.25 M TBABF_4 in 3:1 (v/v) THF/PC (THB), PC (TFP), or 3:1 (v/v) benzonitrile/methylene chloride (TF2P and TF4P). The counter electrode compartments were filled with the same solution without monomer. Prior to each experiment, the platinum electrode was cleaned in a propane flame and then introduced into the working electrode compartment parallel to the glass frits and the counter electrodes. To determine the polymerization potential, the applied potential was increased in 25 mV steps and the current recorded as a function of time. The polymerization potential was determined to be the lowest potential at which a progressive increase in the current was observed over 200–300 s and represents an average of at least three different samples.^{17, 24, 25}

Doping Potentials, Doping Densities, and Cycling Efficiency. The doping potentials, doping densities, and the stability of the polymers were obtained from cyclic voltammetry and the values reported represent the average from at least three different samples. For these experiments, a polymer film was deposited onto a clean platinum electrode at the polymerization potential by passing 100–500 mC cm^{-2} of charge. The corresponding film thicknesses were 1.0–3.5 μm .²⁶ The polymer was then neutralized by scanning the potential to 0.0 V (vs Fc^+/Fc) and then transferred to a clean solution of 0.25 M TBABF_4 in PC and held for 2 h at a constant potential corresponding to the positive potential scan limit used in voltammetry. In all cases, the current decreased exponentially to less than 25 $\mu\text{A cm}^{-2}$ after 2 h. Subsequently, we refer to this electrochemical treatment as postpolymerization.

All voltammograms were acquired at a scan rate of 25 mV s^{-1} , beginning at the open circuit potential. The scan rate of 25 mV s^{-1} was determined to be slow enough to allow complete doping and neutralization of the polymer for the thickness of films deposited.²⁷ The potential limits for cyclic voltammetry were selected to be 100–200 mV beyond the current peak associated with the first n-doping or p-doping wave to give both high doping density and high cycling efficiency.

The stability range for the TBABF_4/PC solution was determined from voltammetry at a platinum electrode. At a scan rate of 25 mV s^{-1} , the potentials at which the background current reached 10 $\mu\text{A cm}^{-2}$ were -3.27 and 1.69 V, respectively. The potential limits used for n- and p-doping of the polymers were, in all cases, within this potential range.

n-Doping and p-doping densities (anodic and cathodic charge capacities, respectively) were calculated from the charge under the neutralization waves in the voltammograms and the mass of the polymer film. The mass of the polymer film was obtained in the following way. A platinum electrode with a neutralized film was rinsed twice in clean THF and vacuum-dried at room temperature for 1 h. After weighing, the polymer film was pyrolyzed in a propane flame and the polymer mass obtained from the difference in mass between the bare substrate and the substrate with polymer. The deposition charge was proportional to the mass of the polymer corresponding to a constant deposition efficiency; however, the deposition efficiencies were different for each monomer.

The cycle-to-cycle stability of the polymer films, S , was calculated from

$$S = 1 - \frac{Q_1 - Q_N}{NQ_1}$$

where N is the number of cycles, and Q_N and Q_1 correspond to

(20) Roncali, J. In *Handbook of Conducting Polymers*, 2nd ed.; Skotheim, T. A.; Elsenbaumer, R. L.; Reynolds, J. R. Eds.; Marcel Dekker: New York, 1998.

(21) Ferraris, J. P.; Guerrero, D. J. In *Handbook of Conducting Polymers*, 2nd ed.; Skotheim, T. A.; Elsenbaumer, R. L.; Reynolds, J. R. Eds.; Marcel Dekker: New York, 1998.

(22) Gritzner, G.; Kuta, J. *J. Pure Appl. Chem.* **1982**, *54*, 527.

(23) Sarker, H.; Gofer, Y.; Killian, J. G.; Poehler, T. O.; Searson, P. C. *Synth. Met.* **1998**, *97*, 1.

(24) Siekierski, M. J.; Przulski, J.; Plochanski, J. *Synth. Met.* **1993**, *61*, 217.

(25) Hillman, A. R.; Mallen, E. F. *J. Electroanal. Chem.* **1987**, *220*, 351.

(26) The film thicknesses were measured using a profilometer (Tencor Alpha Step) on films deposited onto a tin oxide substrate. Due to the inherent difficulties in using profilometry on soft materials, these values are considered estimates.

the charge under the neutralization curve in the N th cycle and the first cycle, respectively.

Spectroscopy. Absorbance spectra were obtained for polymer films deposited onto $20 \Omega/\square$ tin oxide glass (Libby Owens Ford) in a two-compartment electrochemical cell. The cell had an optical path of about 6 cm between a quartz glass window and the tin oxide coated glass substrate. For all experiments, 10 mC cm^{-2} films were polymerized from 0.1 M monomer solution in 0.25 M TBABF₄ in the solvent indicated previously. The polymer film was then electrochemically neutralized and rinsed with a fresh solution of 0.25 M TBABF₄ in PC, and the cell was transferred to the spectrophotometer. The potential was then scanned to the positive potential limit used for voltammetry and held at this potential for up to 2 h during which absorbance spectra were obtained. The spectrophotometer was previously calibrated for baseline and background by recording spectra for the cell in the absence of the polymer film and with clean electrolyte. All spectra are reported after subtracting for the cell and clean electrolyte solution. The instrument was operated in the transmission mode with a 0.5 nm slit width.

Polymer Morphology. The morphology of the polymer films was characterized by scanning electron microscopy (SEM). A 200 mC cm^{-2} polymer film was deposited onto polished platinum foils ($1.5 \times 1.5 \times 0.01 \text{ cm}$) from 0.1 M monomer solution in 0.25 M TBABF₄ in the solvent indicated previously and neutralized. After deposition, the polymer films were immersed in dry PC for 15–30 min and then dried under vacuum at room temperature.

Results and Discussion

Polymerization of the Monomers. The monomer 1,4-bis(2-thienyl)-2-fluorophenylene (TFP) was electropolymerized from TBABF₄/PC solution as an insoluble film on the platinum electrode. The as-polymerized polymer films of poly-TFP were soluble in THF and acetonitrile. The monomers 1,4-bis(2-thienyl)-2,5-difluorophenylene (TF2P) and 1,4-bis(2-thienyl)-2,3,5,6-tetrafluorophenylene (TF4P) were not soluble in PC and were polymerized from a solution of 0.25 M TBABF₄ in benzonitrile/methylene chloride. The films polymerized in this mixed solvent had low solubility, allowing efficient deposition on platinum. For the case of 1,4-bis(2-thienyl)benzene (THB), polymer films were deposited from THF/PC. With all the monomers, the solution in the working electrode compartment acquired an intense green color during the deposition, evidence for the solubility of doped oligomers and/or low molecular weight polymer. We note that polymer films of multiple ring monomers are often characterized by relatively short chain lengths.²⁰

A typical series of current–time curves for the electropolymerization of TFP is shown in Figure 2. For applied potentials lower than the polymerization potential, the current decreased to less than $10 \mu\text{A cm}^{-2}$, similar to the value obtained on platinum in the absence of the monomer. Once the applied potential reached the polymerization potential, a continuous increase in the current was seen after an induction time of 20–300 s. The induction time is related to the slow nucleation kinetics of the polymer, and the increase in current with time is due to the increase in the surface area of the growing polymer. Generally, after several hundred

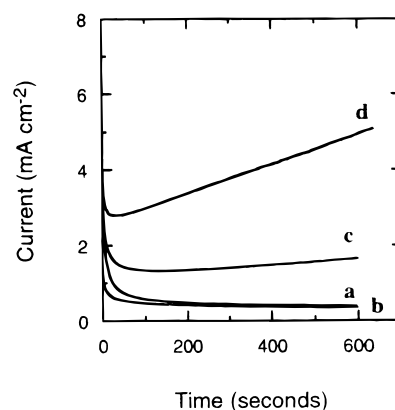


Figure 2. Current time transients at (a) 0.4 V, (b) 0.5 V, (c) 0.675 V, and (d) 0.685 V for 0.1 M TFP monomer in 0.25 M TBABF₄ in PC. The polymerization potential was determined to be 0.675 V.

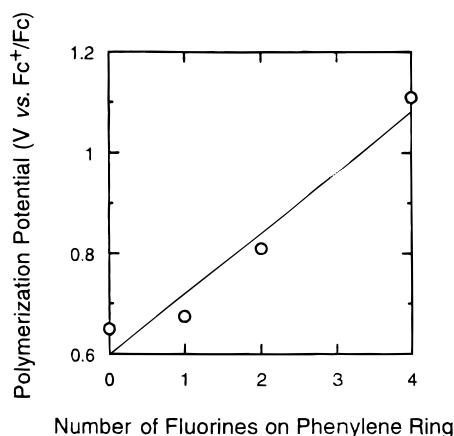


Figure 3. Polymerization potential versus the number of fluorine atoms on the phenylene ring.

seconds, the polymerization current attained a steady-state value corresponding to deposition over a constant surface area.

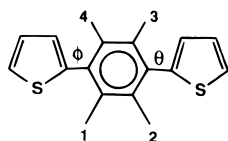
Figure 3 shows the polymerization potential for the four monomers. For convenience these results are plotted versus the number of the fluorine atoms on the phenylene ring. Since polymerization occurs through coupling of the radical cations in the 2 position of the thiophene ring, the electron-withdrawing character of the fluorine substituent is expected to result in higher polymerization potentials with increasing number of fluorine substituents.²⁰ Other groups have shown that the polymerization potentials for many thiophenes substituted in the 3 position increase linearly with the electronic character of the substituent, as characterized by the Hammett constant.^{12,28} In previous work, we have shown that the electropolymerization potential for a series of fluorophenyl thiophenes is also linear with the integrated Hammett constants for the fluorine substituents.¹⁷

For the multiple ring monomers under consideration here, an additional degree of freedom is the dihedral angle between the thiophene and phenylene ring along

(28) Waltman, R. J.; Bargon, J. *Can. J. Chem.* **1986**, *64*, 76.

(29) The dihedral angle was determined for the minimum energy structure of the monomer. All molecular modeling calculations were performed with Spartan 5.0 (Wavefunction, Inc.) using the PM3 basis set.

(27) The doping charge was found to be independent of scan rate at low scan rates, but progressively decreased with increasing scan rate. For all measurements reported here, a 25 mV s^{-1} scan rate was in the region where the doping charge was constant.



Monomer	Substituent	ϕ ($^\circ$)	θ ($^\circ$)
THB	1 = 2 = 3 = 4 = H	36.0	36.0
TFP	1 = 2 = 4 = H, 3 = F	38.0	46.0
T2FP	2 = 4 = H, 1 = 3 = F	46.9	46.9
T4FP	1 = 2 = 3 = 4 = F	89.1	89.1

Figure 4. Dihedral angle between the rings for the four monomers.

Table 1. Electropolymerization Parameters of the Phenylene-2-thienyl Polymers

polyphenylene-2-thienyl	polymerization potential of monomer (V) ^a	polymerization charge (e/mu) ^b	
		as-deposited	as-deposited and postpolymerized
pTHB	0.650	1.46	2.97
pTFP	0.675	1.53	3.51
pTF2P	0.810	1.78	2.75
pTF4P	1.110	2.04	3.18

^a Versus the ferrocene/ferrocenium couple. ^b Electrons per monomer unit.

the monomer backbone. The dihedral angles for the monomers are shown in Figure 4.²⁹ The increase in dihedral angle associated with increasing number of fluorine substituents may result in a distortion of the π -conjugation and hence may influence the reactivity of the monomer or the polymerization potential.^{20,21}

The number of charges needed for polymerization of the monomers was determined from the charge passed during deposition and the mass of the polymer film. In general, for the oxidative polymerization of electronically conducting polymers, the number of electrons for deposition of each monomer unit is expected to be $2 + y + z$ where y is the doping density at the polymerization potential (typically 0.1–0.3 electrons per monomer unit) and z represents the charge associated with parasitic reactions. The factor of 2 assumes the polymerization of relatively long chains; a value of 1.9 would be obtained for a mean chain length of 20 and 1.98 for mean chain length of 100. For polymerization of the monomers reported here, the deposition charge was in the range 1.46–2.04 electrons per monomer unit, as shown in Table 1. These values imply that the as-deposited polymer films have a significant fraction of short chain length oligomers. However, taking into account the additional polymerization charge passed during the postpolymerization treatment (see next section), the polymerization charge increases to 2.7–3.1 electrons per monomer unit (Table 1). This result suggests that significant polymerization of the oligomers occurs during the postpolymerization step, resulting in a much longer mean chain length. We note that an underestimation of the polymer mass due to solubility of oligomers would be expected to result in an overestimate of the deposition charge per monomer.

Figure 5 shows a plan view SEM image of an as-deposited pTFP film illustrating that the film is

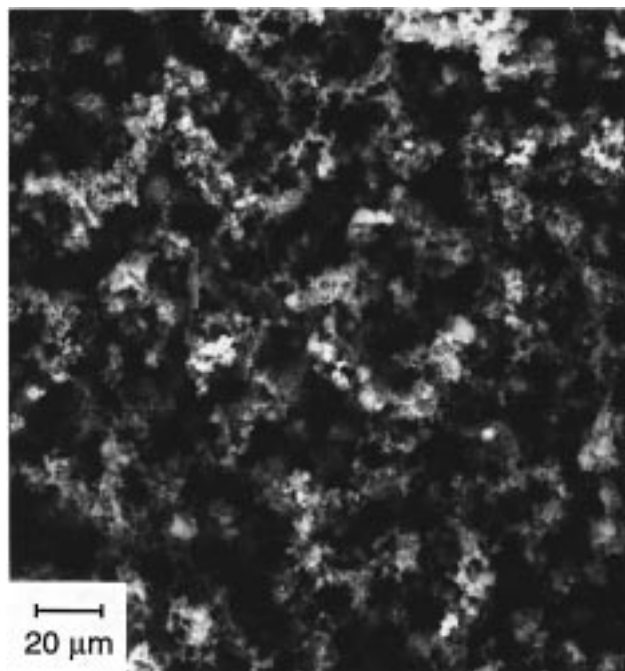


Figure 5. Plan view SEM image of an as-deposited pTFP film illustrating the continuous nature of the film and the characteristic nodular structure.

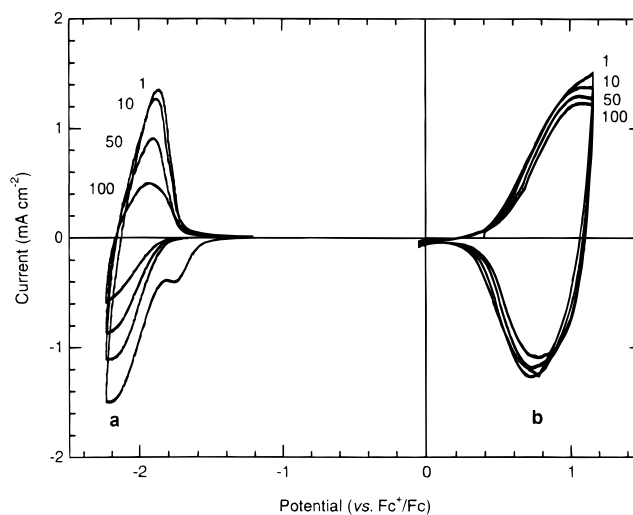


Figure 6. Cyclic voltammograms for pTFP showing the first, 10th, 50th, and 100th cycles for both n-doping (a) and p-doping (b) in 0.25 M TBABF₄ in PC.

continuous, with the nodular structure characteristic of many electronically conducting polymers.^{17,30–32} This indicates that the fraction of long chain lengths is sufficient to allow deposition of a continuous, self-supporting film, since the deposition of short chain length oligomers is usually associated with powdery, discontinuous films.²⁰ Similar results were obtained for all four monomers. Furthermore, no changes in the film morphology were observed after postpolymerization treatment or after multiple p- or n-doping cycles.

Electrochemical Properties of the Polymers. Figure 6 shows voltammograms for the first 100 cycles of p-doping/neutralization and n-doping/neutralization

(30) Coffey, D.; Madsen, P. V.; Poehler, T. O.; Searson, P. C. *J. Electrochem. Soc.* **1995**, *142*, 321.

(31) Bittihn, R.; Ely, G.; Woeffler, F. *Makromol. Chem. Macromol. Symp.* **1987**, *8*, 51.

(32) Osaka, T.; Naoi, K.; Ogano, S.; Nakamura, S. *J. Electrochem. Soc.* **1987**, *134*, 2096.

Table 2. Electrochemical Properties of the Phenylene-2-thienyl Polymers in 0.25 M TBABF₄ in PC

polyphenylene-2-thienyl	n-doping			p-doping		
	peak potential (V) ^{a,b} of polymer			peak potential (V) ^{a,b} of polymer		
	reduction (n-doping)	oxidation (neutralization)	negative voltage limit (V) ^{a,b}	oxidation (p-doping)	reduction (neutralization)	positive voltage limit (V) ^{a,b}
pTHB	-2.16	-2.14	-2.35	0.93	0.77	1.23
pTFP	-2.14	-2.07	-2.27	1.00	0.89	1.15
pTF2P	-2.04	-1.95	-2.25	1.06	0.97	1.26
pTF4P	-2.01	- ^c	-2.22	1.19	1.02	1.34

^a Versus the ferrocene/ferrocenium couple. ^b In 0.25M TBABF₄/PC. ^c Irreversible.

Table 3. Doping Densities and Cycling Efficiencies for the Phenylene-2-thienyl Polymers in 0.25 M TBABF₄ in PC

poly phenylene-2-thienyl	n-doping			p-doping		
	doping density (e/mu) ^{a,b}	charge capacity (mA h g ⁻¹) ^b	charge retained over 100 cycles (%)	doping density (e/mu) ^{a,b}	charge capacity (mA h g ⁻¹) ^b	charge retained over 100 cycles (%)
pTHB	0.12	13.1	6.7	0.45	49.4	70.4
pTFP	0.19	19.7	46.0	0.33	34.4	91.1
pTF2P	0.18	17.2	30.8	0.36	34.4	57.6
pTF4P	- ^c	- ^c	- ^c	-0.15	12.9	59.0

^a Electrons per monomer unit. ^b First cycle. ^c Irreversible.

of pTFP. From this figure it can be seen that pTFP exhibits highly reversible p-doping with only a small decrease in the peak current over 100 cycles. Similar results were obtained for the other polymers.

Table 2 summarizes the potentials of the current peaks associated with the first p- and n-doping waves along with the corresponding neutralization waves. The potential of the p-doping peak increased from 0.93 to 1.19 V and the potential of the n-doping peak increased from -2.16 to -2.01 V with increasing number of fluorines. The band gaps of the polymers, determined from the difference between the potentials corresponding to the onset of the current for p-doping and n-doping,^{1,2,33} increased from 2.08 to 2.63 eV with an increasing number of fluorines.

Table 3 summarizes the results from cyclic voltammetry for the four polymers and shows the doping densities, specific charge capacities, and the charge retained over the first 100 cycles. The doping densities for p-doping were 0.15–0.45 electrons per monomer unit; corresponding to 0.05–0.15 electrons per ring. Although these values are somewhat lower than the values of 0.20–0.30 electrons per ring reported for many electronically conducting polymers, the low molecular weight of the monomers in comparison to many substituted thiophenes^{12,17} results in relatively high charge capacities. For example, the doping density of 0.45 for pTHB corresponds to a charge capacity of 49.4 mA h g⁻¹. In contrast, the doping densities and charge capacities for n-doping were slightly lower, in the range of 0.12–0.19 electrons per monomer unit.

Figure 7 shows the doping characteristics for both p-doping and n-doping. For convenience, these results are plotted versus the number of fluorine atoms on the phenylene ring. This figure shows that the doping densities and potentials corresponding to the peak doping currents are dependent on the number of fluorines. The fluorine substituents can influence the doping properties either directly by modifying the electron withdrawing characteristics of the phenylene ring or

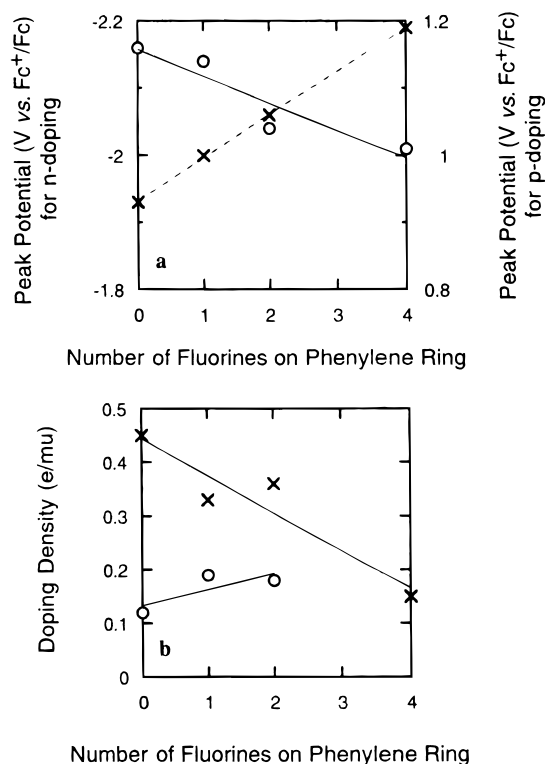


Figure 7. Correlation between the number of fluorine atoms on the phenylene ring and (a) the potential of the current peak for n-doping (○) and p-doping (×) of the polymers, and (b) the doping densities for n-doping (○) and p-doping (×).

indirectly by inducing a change in the dihedral angle and hence distorting the π -conjugation.

For p-doping, where electrons are removed from the π -conjugated system, the increase in electronegativity associated with the increase in the number of fluorine atoms is expected to result in a higher energy barrier for p-doping^{34,35} and hence shift the doping potential peak to more positive values (Figure 7a) and reduce the

(34) Waltman, R. J.; Diaz, A. F.; Bargon, J. *J. Electrochem. Soc.* **1984**, *131*, 1452.

(35) Garcia, P.; Pernaut, J.-M.; Hapiot, P.; Wintgens, V.; Valat, P.; Garnier, F.; Delabouglise, D. *J. Phys. Chem.* **1993**, *97*, 513.

(33) Killian, J. G.; Gofer, Y.; Sarker, H.; Poehler, T. O.; Searson, P. C. to be submitted.

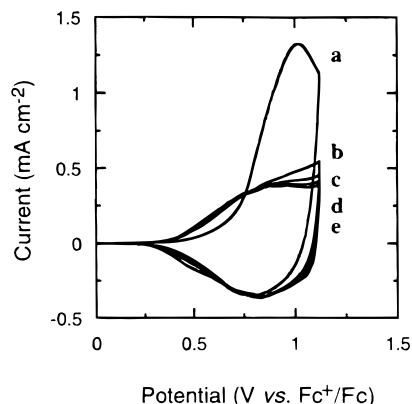


Figure 8. Voltammograms for p-doping/neutralization of 100 mC cm^{-2} pTFP in 0.25 M TBABF_4 in PC. The film was not subjected to a postpolymerization step. The first oxidation wave (a) is much larger than the corresponding neutralization wave. The subsequent cycles (b–e) display a small increase in the neutralization charge. The voltammograms shown here for pTFP are typical of all of the polymers in the series.

doping density (Figure 7b). For n-doping, where electrons are injected into the π -conjugated backbone, the increase in electronegativity associated with the fluorine groups is expected to reduce the energy barrier for n-doping and stabilize the excess negative charge.^{14,36} As seen in Figure 7b, the peak potential for n-doping is shifted to more positive potentials with an increase in the number of fluorine atoms. Enhanced stabilization of the n-doping process has been achieved with pendant groups such as phenyl rings.^{14–17,37} The increase in n-doping density with the number of fluorines for pTHB, pTFP, and pTF2P suggests that the increase in dihedral angle is not significant, since the opposite trend would be expected. The origin of the poor n-doping reversibility for pTF4P is not clear but is consistent with other thiophene moieties with multiple fluorine substituents.¹³ Since the n-doping potential is shifted to more positive values with increasing fluorines, solvent breakdown or reduction of the polymer is unlikely.

Postpolymerization Treatment of the Polymer Films. For the series of four polymers studied here, the p-doping peak potentials were up to 200 mV positive with respect to the polymerization potential, so that as-polymerized films were only partially oxidized. In contrast, for most other conducting polymers, the polymerization potential is positive versus the p-doping peak, resulting in polymerized films which are fully oxidized or even overoxidized.^{12,38,39} As a result, on initial p-doping of the as-polymerized films, further polymerization of polymers and/or short chain oligomers in the film is expected.

Figure 8 shows voltammograms for an as-polymerized film of pTFP showing that the first p-doping peak is significantly larger than the subsequent peaks due to further polymerization of oligomers trapped in the film. Additionally, the doping density obtained from the neutralization waves increases over the first few cycles. The oxidation charge passed during the postpolymer-

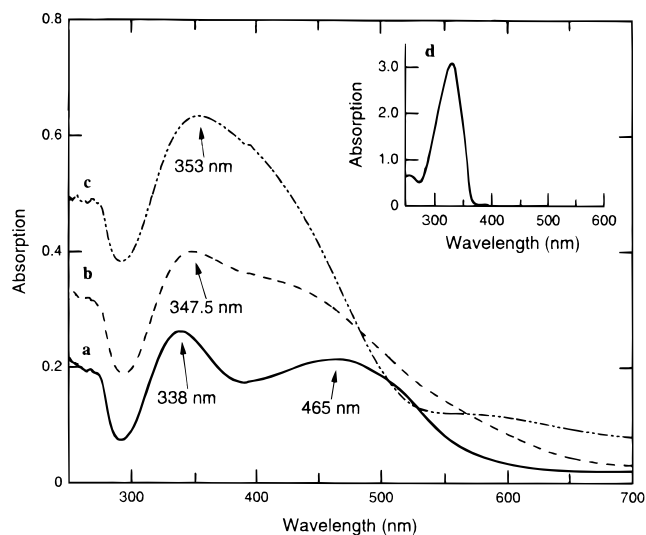


Figure 9. Absorbance spectra for 10 mC cm^{-2} pTFP films on tin oxide glass: (a) as-polymerized, (b) after 45 min at 1.15 V, and (c) after 2 h at 1.15 V. All films were neutralized by scanning the potential to 0 V prior to measurement. For comparison, the inset (d) shows the spectrum for a 0.20 mM solution of TFP monomer in THF. The monomer peak is at 329 nm.

ization step is correlated with the additional charge passed during the first few cycles of as-polymerized films, illustrating that the two processes have the same result.⁴⁰ The decay in the current density during the 2 h postpolymerization step was approximately exponential with a time constant of 85 min, much slower than the doping process, implying that further oxidation of oligomers is only adequately achieved by a constant potential treatment.⁴¹

For all the polymers in this series, the color of the neutral polymer film changed irreversibly from yellow-green to black during the postpolymerization step. Figure 9 shows the absorbance spectra for 10 mC cm^{-2} pTFP films deposited on tin oxide glass. It was found that 10 mC cm^{-2} films were sufficiently transparent for absorption measurements, even after the postpolymerization process. Figure 9a shows an absorbance spectrum for an as-polymerized film after neutralization exhibiting two distinct peaks at 378 and 465 nm. The peak at 338 nm is close to the absorption peak for the monomer at 329 nm (as shown in the inset) and is ascribed to short chain oligomers; the peak at 465 nm corresponds to the main polymer absorption (i.e. long chain lengths). A red shift in the absorbance peak with increasing oligomer length is well-known.^{42,43} After 45

(40) The additional oxidative charge passed during voltammetry was obtained from Figure 8 by subtracting the charge associated with the neutralization of the doped film on the previous cycle from the integrated charge under the p-doping peak. This approach was necessary because each cycle resulted in further polymerization and hence increased the charge associated with the subsequent neutralization. Since the first p-doping cycle does not have a previous neutralization charge, the value of the neutralization charge obtained after polymerization of the film was used.

(41) Although multiple cycles result in an equivalent postpolymerization treatment of the polymer films, the large number of cycles and the slow sweep rate required to complete the process render this method impractical.

(42) Lowry, T.; Richardson, K. S. *Mechanism and Theory in Organic Chemistry*, 3rd ed.; Harper International: New York, 1987; p 981.

(43) Roncali, J.; Garnier, F.; Lemaire, M.; Garreau, R. *Synth. Met.* **1986**, *15*, 323.

(36) Tourillon, G.; Garnier, F. *J. Electroanal. Chem.* **1984**, *161*, 51.

(37) Visy, C. S.; Lukkari, J.; Kankare, J. *Synth. Met.* **1993**, *55–57*, 1620.

(38) Krische, B.; Zagorska, M. *Synth. Met.* **1989**, *28*, C263.

(39) Gratzl, M.; Hsu, D.-F.; Riley, A. M.; Janata, J. *J. Phys. Chem.* **1990**, *94*, 5973.

min at a potential of 1.15 V and subsequent neutralization (Figure 9b), the short chain oligomer peak has shifted to 347.5 nm, suggesting further polymerization of oligomers within the film. Figure 9c shows an absorbance spectrum of a polymer film electrochemically treated at 1.15 V for 2 h in which the short wavelength peak has further shifted to 353 nm. It should be noted that the absorption peak at 465 nm blue shifts during this process, suggesting that the absorption coefficient of the oligomers becomes very high in relation to the polymer and/or overoxidation of the polymer occurs.

In summary, the oxidation charge passed during the initial 2 h, postpolymerization process is due to both p-doping of the polymer and oligomer-oligomer polymerization. This process increases the average chain length in the film, producing an increase in the doping density upon neutralization consistent with an increase in polymer conjugation length. The polymerization efficiency and the bathochromic shift in the absorption spectra support this conclusion. We note that similar increases in p-doping density during voltammetry have been reported for polythiophene-based polymers,⁴⁴⁻⁴⁸ particularly for multiple ring thiophene moieties,^{43,49-51} and have been ascribed to "activation" or "break in" of the polymer film.

The constant potential postpolymerization treatment was found to influence the n-doping of the polymer films. Neutral polymer films that were subjected to n-doping/neutralization without the postpolymerization step exhibited very poor cycling efficiency. The charge under the neutralization waves decreased dramatically after 2 cycles for pTFP and after 10 cycles for pTHB, resulting in cycling efficiencies on the order of 90-95% per cycle. For the case of pTFP, the decrease in the neutralization charge was associated with a complete removal of the polymer film from the substrate and discoloration of the solution. In contrast, pTFP and pTHB films that were subjected to the postpolymerization step before cycling in the n-doping regime exhibited higher initial n-doping levels and greatly enhanced cycling efficiencies. The treated films turned black and, when cycled 100 n-doping/neutralization cycles, remained on the surface with no change in color and only slight discoloration of the solution. It is interesting to note that films of pTFP and pTHB which had undergone n-doping/neutralization cycling without postpolymerization treatment subsequently exhibited higher p-doping densities comparable to films that had been subjected to the postpolymerization step.

Fabrication and Testing of Charge Storage Devices. On the basis of the results obtained from single electrode measurements, we have constructed prototype cells with poly-3-(3,4,5-trifluorophenyl)thiophene (pT-

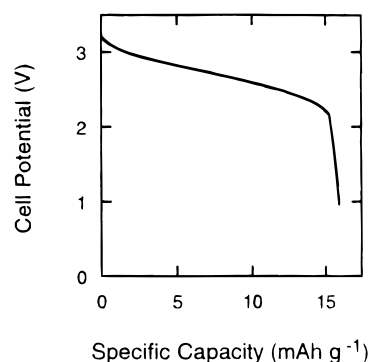


Figure 10. Specific capacity for a cell constructed from a pTFP cathode and a pTFPT anode. The inset shows the corresponding charge (---)/discharge (—) curve. The current density for charge and discharge was $250 \mu\text{A cm}^{-2}$ and the voltage limits were 3.25 V and 1.0 V.

FPT) anodes and pTFP cathodes. These two polymers provide a high charge capacity along with good cycling efficiency. Films of the polymers were deposited onto 4 cm^2 platinum foil current collectors in a two-compartment cell, in which the counter electrode compartment was separated from the working electrode compartment by a large glass frit. Deposition charges of $0.5-5 \text{ C cm}^{-2}$ were employed with careful matching of the charge capacity of the individual anode/cathode pairs. After deposition, neutralization, and postpolymerization treatment (for pTFP) of the polymer, electrodes were placed in clean 0.25 M TBABF_4 in PC in a two-electrode cell configuration. Some of the test cells were constructed to function in a cathode limited mode (10% difference) to account for the lower cycling efficiency associated with n-doping. Several cells were assembled and tested over multiple constant current charge/discharge cycles varying from 40 to $500 \mu\text{A cm}^{-2}$.

Figure 10 shows a typical discharge curve for a cell charged at a constant current density of $250 \mu\text{A cm}^{-2}$ to a cutoff voltage of 3.25 V, held at the cutoff voltage for 2 h or until the current density decreased to less than $62.5 \mu\text{A cm}^{-2}$, followed by discharge at $250 \mu\text{A cm}^{-2}$ to 1 V. As seen in Figure 10, the discharge voltage versus time curve exhibits an extended voltage plateau with an average cell potential of about 2.75 V, followed by a sharp drop in the potential close to the point of complete discharge. These operating voltages are higher than for traditional aqueous charge storage devices and are approaching values for lithium-based battery systems.⁵² The average specific charge and specific energy of the test cells were 17.5 mA h g^{-1} , and 33.4 mW h g^{-1} , respectively, based on the mass of the neutral active polymers. The average cycling efficiency obtained over 100-150 cycles was 99.14% per cycle. The specific charge corresponds to about 99.5% of the maximum value expected from the three electrode measurements.

Conclusions

We have characterized the electrochemical properties of a series of four fluoro-substituted phenylene-2-thienyl polymers. The polymerization potential for all four monomers was negative with respect to the first p-

(44) Kawai, T.; Iwasa, T.; Onada, M.; Sakamoto, T.; Yoshino, K. *J. Electrochem. Soc.* **1992**, *139*, 3404.

(45) Novák, P.; Müller, K.; Santhanam, K. S. V.; Haas, O. *Chem. Rev.* **1997**, *97*, 207.

(46) Arbizzani, C.; Mastragostino, M. *Electrochim. Acta* **1990**, *35*, 251.

(47) Corradinni, A.; Mastragostino, M. *Synth. Met.* **1987**, *18*, 625.

(48) Grimshaw, J.; Perera, S. D. *J. Electroanal. Chem.* **1990**, *278*, 287.

(49) Zotti, G.; Schiavon, G. *Synth. Met.* **1990**, *39*, 183.

(50) Roncali, J.; Gorgues, A.; Jubault, M. *Chem. Mater.* **1993**, *5*, 1456.

(51) Visy, C.; Lukkari, J.; Kankare, J. *Macromolecules* **1994**, *27*, 3322.

(52) Linden, D. In *Handbook of Batteries*, 2nd ed.; Linden, D., Ed.; McGraw-Hill, Inc.: New York, 1995; Chapter 23.

doping peak of the polymer. This feature results in incomplete polymerization of oligomers in the film. Complete polymerization of oligomers in the film was achieved by a postpolymerization step prior to further electrochemical measurements. The doping properties of the polymer films were dependent on the electronic and steric effects arising from the fluorine substituents on the phenylene ring. The polymers pTHB, pTFP,

pTF2P all exhibited reversible n-doping and p-doping.

Cells utilizing a poly-1,4-bis(2-thienyl)-2-fluorophenylene cathode and a poly-3-(3,4,5-trifluorophenyl)thiophene anode were constructed. It was shown that the cells display a maximum voltage of 3.25 V and a specific capacity of 17.5 mA h g⁻¹ (specific energy of 33.4 mW h g⁻¹).

CM981042D